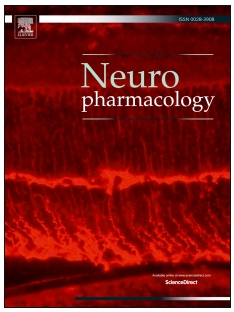

Serotonin (5-HT) neuron-specific inactivation of Cadherin-13 impacts 5-HT system formation and cognitive function

Andrea Forero, Hsing-Ping Ku, Ana Belen Malpartida, Sina Wäldchen, Judit Alhama-Riba, Christina Kulka, Benjamin Aboagye, William.H.J. Norton, Andrew.M.J. Young, Yu-Qiang Ding, Robert Blum, Markus Sauer, Olga Rivero, Klaus-Peter Lesch

PII: S0028-3908(20)30084-8

DOI: https://doi.org/10.1016/j.neuropharm.2020.108018

Reference: NP 108018

To appear in: *Neuropharmacology*

Received Date: 5 September 2019

Revised Date: 15 February 2020

Accepted Date: 23 February 2020

Please cite this article as: Forero, A., Ku, H.-P., Malpartida, A.B., Wäldchen, S., Alhama-Riba, J., Kulka, C., Aboagye, B., Norton, W.H.J., Young, A.M.J., Ding, Y.-Q., Blum, R., Sauer, M., Rivero, O., Lesch, K.-P., Serotonin (5-HT) neuron-specific inactivation of Cadherin-13 impacts 5-HT system formation and cognitive function, *Neuropharmacology* (2020), doi: https://doi.org/10.1016/j.neuropharm.2020.108018.

Serotonin (5-HT) neuron-specific inactivation of Cadherin-13 impacts 5-HT system formation and cognitive function

Andrea Forero[1,a], Hsing-Ping Ku[1,a], Ana Belen Malpartida[1], Sina Wäldchen[2], Judit Alhama-Riba[1], Christina Kulka[1], Benjamin Aboagye[1], William H J Norton[3], Andrew M J Young[3], Yu-Qiang Ding[4], Robert Blum[5], Markus Sauer[2], Olga Rivero[1,b], Klaus-Peter Lesch[1,5,6,b]

Affiliations:

[1]Division of Molecular Psychiatry, Center of Mental Health, University of Würzburg, Würzburg, Germany.

[2]Department of Biotechnology and Biophysics, Biocenter, University of Würzburg, Würzburg, Germany.

[3]Department of Neuroscience, Psychology and Behaviour, University of Leicester, Leicester, UK.

[4]Institute of Brain Sciences, Fudan University, Shanghai, 200031, China.

[5]Institute of Clinical Neurobiology, University of Würzburg, Würzburg, Germany.

[6]Laboratory of Psychiatric Neurobiology, Institute of Molecular Medicine, Sechenov First Moscow State Medical University, Moscow, Russia.

[7]Department of Psychiatry and Neuropsychology, School for Mental Health and Neuroscience (MHeNS), Maastricht University, Maastricht, The Netherlands.

[a] These authors contributed equally

[b] These authors jointly supervised this work

Correspondence:

Andrea Forero
Division of Molecular Psychiatry
Center of Mental Health
University of Würzburg
Margarete-Höppel-Platz 1
97080 Würzburg, Germany

Phone: +49 931 201 77240
E-mail: andrea.forero@stud-mail.uni-wuerzburg.de

Klaus-Peter Lesch, M.D.
Division of Molecular Psychiatry
Center of Mental Health
University of Würzburg
Margarete-Höppel-Platz 1
97080 Würzburg, Germany

Phone: +49 931 201 77600
E-mail: kplesch@mail.uni-wuerzburg.de
Website: www.molecularpsychiatry.ukw.de

Abstract (195 words)

Genome-wide screening approaches identified the cell adhesion molecule Cadherin-13 (CDH13) as a risk factor for neurodevelopmental disorders, nevertheless the contribution of CDH13 to the disease mechanism remains obscure. CDH13 is involved in neurite outgrowth and axon guidance during early brain development and we previously provided evidence that constitutive CDH13 deficiency influences the formation of the raphe serotonin (5-HT) system by modifying neuron-radial glia interaction.

Here, we dissect the specific impact of CDH13 on 5-HT neuron development and function using a 5-HT neuron-specific *Cdh13* knockout mouse model (conditional *Cdh13* knockout, *Cdh13* cKO).

Our results show that exclusive inactivation of CDH13 in 5-HT neurons selectively increases 5-HT neuron density in the embryonic dorsal raphe, with persistence into adulthood, and serotonergic innervation of the developing prefrontal cortex. At the behavioral level, adult *Cdh13* cKO mice display delayed acquisition of several learning tasks and a subtle impulsive-like phenotype, with decreased latency in a sociability paradigm alongside with deficits in visuospatial memory. Anxiety-related traits were not observed in *Cdh13* cKO mice.

Our findings further support the critical role of CDH13 in the development of dorsal raphe 5-HT circuitries, a mechanism that may underlie specific clinical features observed in neurodevelopmental disorders.

Key words: Serotonin (5-HT); Raphe nucleus; Cadherin-13; cell adhesion molecules; neurodevelopment; learning and memory.

1. Introduction

Cadherin-13 (CDH13) is a calcium-dependent cell adhesion molecule that has been reported as a risk factor for neurodevelopmental and psychiatric disorders, including attention-deficit/hyperactivity disorder (ADHD) and autism spectrum disorder (ASD) (for review see: Hawi et al. (2018); Rivero et al. (2013) as well as major depression (Howard et al., 2019). CDH13 regulates a wide range of cellular processes in early brain development, in particular neurite outgrowth and axon guidance, as shown in motor neurons as well as thalamocortical projections (Ciatto et al., 2010; Fredette, Miller, & Ranscht, 1996; Fredette & Ranscht, 1994; Hayano et al., 2014; Ranscht & Bronner-Fraser, 1991). CDH13 also plays a key role in GABAergic function, by contributing to the formation and functioning of inhibitory synapses (Paradis et al., 2007; Rivero et al., 2015; Tantra et al., 2018). Finally, it is acting as a protective factor in the development of cortical interneurons (Killen et al., 2017).

Moreover, the neurodevelopmental involvement of CDH13 extends to monoaminergic systems. The serotonin (5-HT) system, composed of nine raphe nuclei located along the mouse midbrain-hindbrain axis, constitutes an important modulator in diverse cellular processes including cell migration, proliferation and differentiation (Deneris & Gaspar, 2018; Gaspar, Cases, & Maroteaux, 2003). Serotonin signaling is also critical for the development of other neurotransmission systems in the brain (Whitaker-Azmitia, 2001). The most rostral raphe nuclei, the dorsal and median raphe, mediate diffuse serotonergic innervation of anterior regions of the brain that are involved in executive function, impulsive control and anxiety (Dalley & Roiser, 2012; Kiyasova & Gaspar, 2011). Recently, we have been exploring the contribution of CDH13 to the development of these nuclei (Forero et al., 2017). CDH13 is strongly expressed in 5-HT neurons of the dorsal raphe (DR) nucleus both in the embryonic and adult mouse brain (Forero et al., 2017; Rivero et al., 2013). Specifically, CDH13 was detected in 5-HT positive neurons as well as in radial glial cells in the developing hindbrain at early stages of neurodevelopment, starting at embryonic day (E)13.5 (Forero et al., 2017). 5-HT neurons were found to be intertwined in radial glial cells and CDH13-positive clusters were identified at the intersection points between these two cell types suggesting a potential role of CDH13 in the migration of serotonergic neurons (Forero et al., 2017). As CDH13 has previously been linked to cellular migration in non-neuronal cells (Philippova et al., 2005), *Cdh13* knockout mice present an increase in 5-HT neuron density of the DR nucleus at embryonic stages and in adulthood. In addition, serotonergic hyperinnervation of the embryonic prefrontal cortex was detected (Forero et al., 2017).

In the present study, we aimed to elucidate the relationship between CDH13 and the 5-HT system. Recent studies indicated that there is a high specificity in the brain regions each raphe 5-HT neuron subpopulation projects to (Deneris & Gaspar, 2018; Kiyasova & Gaspar, 2011; Muzerelle, Scotto-Lomassese, Bernard, Soiza-Reilly, & Gaspar, 2016; Okaty et al., 2015; Ren et al., 2018). We therefore generated a conditional knockout mouse line where *Cdh13* is selectively eliminated from Pet1-expressing neurons. Pet1 is a transcription factor that is required for the acquisition of serotonergic identity and expression of serotonergic genes in all 5-HT neurons of the raphe nuclei (Hendricks et al., 2003; Kiyasova et al., 2011; Wyler,

Donovan, Yeager, & Deneris, 2015; Wyler et al., 2016). Using this novel 5-HT neuron-specific *Cdh13* knockout mouse model (*Cdh13*$^{loxP/loxP}$::*Pet1-Cre*$^{+/-}$; *Cdh13* cKO), we conducted a detailed characterization of the expression of CDH13 in neuronal subpopulations of the DR and further clarified the specific impact of CDH13 on 5-HT neuron development and function. Our data show that the selective removal of CDH13 from serotonergic neurons impairs cellular properties of the serotonergic projection neurons and also affects learning-related behavior.

2. Methods

2.1. Generation of a serotonin neuron-specific *Cdh13* knockout mouse

All experimental procedures were approved by the boards of the University of Würzburg and the Government of Lower Franconia (55.2-2531.01-92/13) and performed in accordance with the guidelines for animal care and use provided by the European Community. All mice were housed in groups of 3-5 per cage at the facility of the Center of Experimental Molecular Medicine, University Hospital of Würzburg, under a 12 h light/dark cycle with food and water *ad libitum* unless specified otherwise. Mice were kept on a C57Bl/6N background.

The 5-HT neuron-specific *Cdh13* knockout (*Cdh13*$^{loxP/loxP}$::*Pet1-Cre*$^{+/-}$ in the following referred to as *Cdh13* cKO) was generated by subsequently crossing *Cdh13*$^{loxP/loxP}$ mice (Rivero et al., 2015) with *Pet1-Cre* mice. *Pet1-Cre* deleter mice express Cre recombinase under the control of the *Pet1* promoter (Dai et al., 2008). Once established, the mouse line was maintained by breeding *Cdh13*$^{loxP/loxP}$ animals that were negative for Cre (in the following referred to as Ctrl) with *Cdh13* cKO mice (*Cdh13*$^{loxP/loxP}$::*Pet1-Cre*$^{+/-}$). The genotyping of *Cdh13* and *Cre* loci was done by polymerase chain reaction (PCR) (Rivero et al., 2015). The absence of CDH13 from serotonergic neurons was verified by immunohistochemistry and microdissection of the dorsal raphe followed by quantitative real time PCR (qRT-PCR) as described below and in the Supplementary Information section.

2.2.Tissue preparation

*Embryo*s. Ctrl females were crossed with *Cdh13* cKO males to obtain Ctrl and *Cdh13* cKO embryo littermates to be used for histological analysis. Embryos were extracted at developmental stages E13.5 and E17.5. For stage E13.5 the complete head was processed. The brains from E17.5 embryos were dissected from skull. A small sample of the most caudal part of each embryo was taken for genotyping of the *Cdh13* and *Cre* loci (Rivero et al., 2015). Fixation of brains was done by immersion in 4% paraformaldehyde (1x PBS; pH 7.4) at 4°C for 24 h, followed by cryoprotection in 10% and 20% sucrose solutions for one day each, consecutively. The brains were frozen in isopentane cooled with dry ice. Sagittal 20 µm -thick cryosections were mounted on Histobond®+ adhesive microscope slides (Paul Marienfeld, Lauda-Königshofen, Germany). Sections were finally stored at -80°C.

Adults. At an age of 3-4 months mice were sacrificed with isoflurane and subjected to transcardial perfusion. The perfusion consisted of an initial prewash using heparinized PBS (20 units/mL) for 11 min followed by 11 min of ice-cold 4% paraformaldehyde (1xPBS; pH 7.5) at a flow rate of 2.75 mL/min. Brains were dissected and postfixed in 4% paraformaldehyde (1× PBS; pH 7.5) for 48 h, and consecutively placed in 10 and 20% sucrose solutions for one day each. The brains were then frozen in isopentane cooled with dry ice and cryosectioned in coronal or sagittal 20 µm-thick sections.

2.3.Indirect immunofluorescence

Brain sections were allowed to air dry for 45 min at room temperature and were then washed in 1× TBS. For antigen retrieval, sections were treated with citrate buffer (10 mM, pH 6.0) at 80°C in a water bath. Blocking solution (10% horse serum and 0.2% Triton X-100 in 1× TBS) was then applied for 1 h. Next, sections were incubated overnight at 4°C in a wet chamber

with one or two of the following primary antibodies: polyclonal goat anti-Cdh13 (1:400, R&D Systems, Minneapolis, USA, cat# AF3264), polyclonal rabbit anti-5-HT (1:1000, Acris, Herford, Germany, cat# 20080), rabbit anti-serotonin (5-HT) transporter (1:500, Merck Millipore, cat# PC177L), and/or rabbit anti-tryptophan hydroxylase 2 (TPH2) (1:1,000; generated and validated as reported in Gutknecht, Kriegebaum, Waider, Schmitt, and Lesch (2009); Gutknecht et al. (2008)). The next day, sections were washed with 1× TBS and incubated at room temperature with the corresponding secondary antibodies, donkey anti-goat IgG (H+L) Alexa Fluor 555, donkey anti-mouse IgG (H+L) Alexa Fluor 488, and/or donkey anti-rabbit IgG (H+L) Alexa Fluor 488. DAPI (4′,6-diamidin-2-phenylindol) was applied as a nuclear counterstain. Finally, sections were embedded in Fluorogel (Electron Microscopy Sciences, Hatfield, USA) as mounting medium.

2.4.Imaging

Stained sections were imaged with one of the following microscopy techniques: confocal microscopy or structured illumination microscopy (SIM).

Confocal microscopy. Confocal microscopy was carried out as specified in Forero et al. (2017). A FluoView FV1000 confocal microscope (Olympus, Tokyo, Japan) with 20×/0.75 UPlanSAPO objective was used. Raw images (12-bit) were processed with the imaging software Fluoview, version 4.1.a (Olympus).

Structured illumination microscopy. SIM was conducted as reported in Forero et al. (2017). A commercial inverted SIM microscope (Zeiss ELYRA, Oberkochen, Germany) using an oil-immersion objective (Plan-Apochromat 63×/1.4 oil Dic M27) (Gustafsson, 2000; Wegel et al., 2016) was used to capture the images. Recorded data were processed with the ZEN imaging software (Zeiss).

2.5.Cell density quantification in dorsal raphe nuclei

Embryos. The cell density of serotonergic neurons in the DR was analysed at E13.5 by an observer unaware of genotype. The complete DR was imaged using a FluoView FV1000 confocal microscope (Olympus) with 20×/0.75 UPlanSAPO objective. In each image, the DR was selected as the region of interest (ROI) and then the ‘Cell Counter’ plug-in (ImageJ) was used to count 5-HT immunoreactive cells. The DAPI counterstain was used to ensure that only those cells with a visible and focused nucleus were counted, in order to avoid double counts. Then the average number of cells for each brain was determined. In addition, the area of the ROI was also determined using the ‘Measure’ plug-in on ImageJ.

Adults. In adult brains, the density of serotonergic neurons in the DR was determined for each of its three main subregions: (1) dorsal (B7d), (2) ventral (B7v) and (3) lateral (B7l). Images from three to four sections at intervals of 120 μm were taken with a confocal microscope, as described above. The images were then processed using ImageJ. The background was subtracted with a rolling ball value of 20, and the image palette was changed to “Fire” to better identify TPH2-immunoreactive cells. The number of cells for each subcomponent was counted, and the mean number of TPH2-positive cells was calculated for each brain.

2.6. Serotonergic innervation in target regions

Embryos. The prefrontal cortex and the somatosensory cortex were imaged at E17.5 with a confocal microscope as described above. The intermediate zone (IZ), where the serotonergic fibers are located at this developmental stage, was selected as the ROI. In order to make the 5-HT immunoreactive fibers clearly distinguishable from the background, image background was removed using the 'Subtract background' function on ImageJ with 'Rolling' values of 5, 10 and 15 consecutively. Images were made binary and a rectangle of 79.5 μm × 636 μm surrounding the IZ was drawn. Having selected the ROI, 5-HT immunoreactive fibers were counted using the 'Analyze particles' ImageJ function. The total area (number of pixels) occupied by the 5-HT immunoreactive fibers was calculated. The analysis was automated using a script.

Adults. The serotonergic innervation of several target regions was also analyzed in adult brains. The regions were the following: (1) prefrontal cortex (including cingulate and infralimbic cortices), (2) thalamus (including median and lateral thalamus), (3) caudate putamen, and (4) amygdala. These regions were previously identified as the main target regions of the lateral (B7l) and ventral (B7v) DR (Muzerelle et al. (2016). Each region was imaged by confocal microscopy for 3-4 times per brain hemisphere. Section interval was 120 μm. The images were processed using ImageJ. Initially the background was subtracted with a "Rolling ball" value of 1.45 or 1.5 depending on the region (Supplementary Table S1). Then the contrast was enhanced, and the image was made binary allowing only immunostained elements to be visible. A section was selected in the center of the image (Supplementary Table S1), and the area (total number of pixels) occupied by the 5-HTT positive fibers was measured using the "Analyze Particles" option in each individual image.

2.7. Behavioral Assessment

To better understand whether CDH13 deficiency in the serotonergic network affects mouse behavior, we investigated the behavioral repertoire in the *Cdh13* cKO mice. Due to the relationship between *CDH13* and neurodevelopmental disorders ADHD and ASD (for review see: Hawi et al. (2018); Rivero et al. (2013)), we aimed to use behavioral tests that are typically used to investigate impulsivity, attention, cognitive abilities and sociability. Anxiety-like behavior was also tested, because anxiety has been identified as a comorbidity of ADHD (Schatz & Rostain, 2006). To this end, a cohort of adult male *Cdh13* cKO mice (n=8-14) and their Ctrl littermates (n=8-10) were subjected to a series of behavioral tests from 3-4 months of age to assess anxiety-like behavior (elevated plus maze, light-dark box, open field), sociability and preference for social memory (social interaction test), locomotor activity (open field test) as well as visuospatial learning and memory and cognitive flexibility (Barnes maze test). In addition, a second cohort of male *Cdh13* cKO mice (n=13) and Ctrl littermates (n=7) was subjected to the 5-choice serial reaction time task (5-CSRTT) from 4-5 months of age to evaluate attention and impulsivity (Robbins, 2002).

Behavioral testing was performed during the light cycle between 9 am and 5 pm. The behavior was recorded and analyzed using VideoMot2 software (TSE Systems) unless otherwise specified. The examiner was blinded to the genotypes. The order in which the tests were carried out was from least to most stressful and was as described above.

All the tests were conducted as previously described by Rivero et al. (2015) with minor modifications.

Open field. The open field (OF) test was performed to measure locomotor activity as well as anxiety-like behavior. The OF is composed of a square box semi-permeable to infrared light (50×540 cm) with an illumination gradient between 50 and 100 lx from the walls to the center of the arena. The mice were placed individually in one of the corners of the arena and their movement was monitored for a duration of 30 min using a CCD camera positioned above the center of the setup. The total distance traveled as a measure of locomotor activity, as well as the amount of time spent in the central and border areas and the latency to enter the center of the arena as measures for anxiety-like behavior were then calculated.

Elevated plus maze. The elevated plus maze (EPM) was used to assess anxiety-like behavior. The mice were placed in the center of the maze which consists of an elevated platform approximately 60 cm above the floor, with two open arms (illumination of 50 lx) and two closed, dark arms (15 cm high walls, illumination of 5 lx), each arm with a dimension of 30×5 cm and semi-permeable to infrared light (TSE Systems, Bad Homburg, Germany). Animals were allowed to explore the maze for 10 min, during which the animals' trajectory was tracked using a CCD camera. The videos were then analyzed in order to calculate the number of entries, the latency to enter, and the time spent in each of the arms as well as the total distance traveled.

Light-dark box. The light-dark box (LDB) test also allows the evaluation of anxiety-like behavior. The apparatus consists of a square box (50×50×40 cm) semi-permeable to infrared light that contains a black insert measuring one third of the total area of the box with a small opening that allows access to the rest of the box. The illumination of the light compartment is approximately 100 lx, while the illumination of the dark compartment is between 0 and 5 lx. Each mouse was individually placed in the dark compartment and its movement was tracked for 10 min. The number of entries and the latency to enter the lit compartment, as well as the time spent in each compartment were analyzed as measures of anxiety-like behavior. Total distance travelled was also recorded.

Barnes maze. The Barnes maze (BM) was performed to evaluate visuospatial learning and memory. The testing apparatus (TSE Systems) consists of a circular grey platform (120 cm in diameter) with 40 holes around its circumference (each 5 cm in diameter); one of the holes was randomly chosen to hold an escape box. Visual cues to allow visuospatial orientation were located around the maze at a distance of approximately 10 cm. At each trial, the mice were individually placed in the center of the maze and covered with a start cylinder. After removing the cylinder, mice were allowed to explore the maze and behavior was recorded until the mouse found the escape hole. If the mouse was unable to find the escape hole within 3 min, the mouse was carefully guided to the escape hole. Mice were trained to find the hidden escape box for 9 days (2 trials per day), with a resting period of 24 h between days 4 and 5. The latency to start exploring, latency to escape as well as the total distance travelled were automatically measured by the VideoMot2 software. The number of primary errors,

defined as the number of times the mouse poked its head into a wrong hole before the first encounter with the escape hole, were manually scored. The time spent in each quadrant was analyzed by dividing the maze into four equal quadrants consisting of 10 holes, with the target hole approximately in the center of the target quadrant. The other quadrants were labeled clockwise from the target quadrant as positive, opposite, and negative (Attar et al., 2013).

Two-trial social interaction test. The social interaction test was performed in the OF arena to which the animals had already been habituated. This test measures both sociability and preference for social novelty in two consecutive trials. In the first trial (sociability test), the mice were placed in the arena for 10 min and were given the opportunity to explore either an unfamiliar mouse that was enclosed in a small plastic grid cage or an identical empty plastic grid cage. The small cages were located in the upper left and right corners of the arena and the positions of the cage with the unfamiliar animal and the empty cage were randomly alternated between trials to prevent possible effects of side preference. During the second trial that was performed 5 min later (test of preference for social novelty), the mice were placed in the arena and were given the choice to explore the first, now familiar mouse, or a novel, unfamiliar mouse, both enclosed in small plastic cages. The behavior was recorded, and measurements of the total distance traveled, the number of visits and time spent within each interaction zone (animal vs cage; familiar animal vs novel animal), as well as the latency to explore each, were taken. Sociability was defined as interaction time with an unfamiliar mouse over an empty cage. Preference for social novelty was defined as time spent interacting with the novel mouse over the familiar mouse.

Five-choice serial-reaction time task. Visuospatial attentional performance and motor impulsivity was assessed using the five-choice serial-reaction time task (5-CSRTT). The operant chamber was placed within a ventilated, illuminated and sound-attenuating box (5-Hole Box Systems, TSE Systems, Homburg, Germany). The rear wall of the chamber was curved and incorporated five equally spaced apertures as well as food dispensers. Inside each of these apertures was a stimulus light, used to illuminate the hole, and an infrared beam detector for monitoring nose-pokes by the mouse. A timeout signal lamp was mounted above the front nose-poke hole (H6), which was also monitored by an infrared sensor. The presentation of the light stimuli was controlled by the TSE Operant behavior software; the recording of the animals' responses was captured with a CCD camera mounted on the ceiling of the box.

During the whole duration of the test, mice were food-restricted and maintained at 85-90% of their free-feeding body weight, with their target weights adjusted upward every week by 1 g to account for growth. Food restriction started one week before the beginning of the test; water was available *ad libitum* at all times.

The task was divided in three main phases, habituation, autoshaping and testing, which included two testing levels and a variable inter-trial interval (vITI) challenge. Mice were familiarized with the 5-CSRTT chamber and trained to associate nosepoking into a lit aperture with reward during habituation phase. The major training period is termed autoshaping. It is when the mice were trained step by step to perform the task by learning to discriminate between rewarding nose-pokes (lit holes) and those that did not lead to a reward

(unlit holes) as well as to perform over a longer period of time in the chamber. After the mice had reached criteria (>75% accuracy, <15% omission for three consecutive days) at 10-s stimulus duration (StD) and 10-s inter-trial interval (ITI) within the last autoshaping level, mice were probed for attention and impulse control deficits at 5 and 2 s stimulus durations during the testing phase. Additionally, to make it unpredictable for the animals, 2 sessions of challenge (vITI) encompassing varying the ITI between 6 and 14 s that was presented randomly by the TSE operant behavior system software were carried out. Attentional performance was recorded, and measurements of the correct response, incorrect response, premature response, omission, latencies to correct and incorrect responses, reinforcers earned, the number of completed trials, and nose-pokes at each aperture were taken. The accuracy and the total number of nose-pokes were calculated from the raw data. For the detailed experimental procedure, the parameters of each specific levels and the definition of parameters see supplementary material.

2.8.Statistical analysis

The normality of the data sets was verified using the Kolmogorow-Smirnov test and Shapiro-Wilk test. Once a normal distribution was confirmed, genotype effects were analyzed by a two-tailed unpaired *t*-test, otherwise the nonparametric Mann-Whitney test was conducted. For those behavioral tests with repeated measures (i.e. BM and 5-CSRTT), a repeated-measures mixed analysis of variance was used, with genotype as between-subject factor and test session as the repeated measure. Animals that were statistically identified as outliers were excluded from the analysis. A Sidak post-hoc test was used to follow up significant main effects and interactions. For the 5-CSRTT, an additional Tukey post-hoc test was carried out to assess the learning progress by comparing the performance of each individual genotype among sessions during the testing phase. Statistical analyses were performed using Prism, version 7.0a (GraphPad Software, La Jolla, CA, USA) and/or SPSS Statistics, version 25.0 (IBM Corp., Armonk, NY).

3. Results

3.1. Conditional *Cdh13* inactivation in Pet1-positive neurons increases cell density in the developing dorsal raphe nucleus

We aimed to study how the specific expression of CDH13 in serotonergic neurons contributes to the altered phenotypes observed in constitutive *Cdh13* knockout embryos. We generated a conditional knockout mouse line where CDH13 is selectively eliminated from *Pet1* expressing neurons (Dai et al., 2008). Pet1 is a transcription factor that is required for the acquisition of serotonergic specification and is active during the development of serotonergic neurons in the raphe nuclei ((Kiyasova et al., 2011). As shown in Figure 1A, immunofluorescence staining of both CDH13 and 5-HT in combination with super-resolution imaging by structured illumination microscopy (SIM) (Gustafsson, 2000) confirmed a considerable decrease of CDH13 in the DR of *Cdh13* cKO mice, compared to Ctrl mice. Additionally, super-resolution microscopy at single 5-HT positive neurons in *Cdh13* cKO embryos revealed that CDH13 does not appear to cluster in the extending neurites or soma of these cells, as it was observed in Ctrl mice (Fig. 1B). We still observe traces of CDH13 immunoreactivity close to serotonergic, 5-HT-positive neurons, most likely coming from adjacent cells, such as radial glia (Forero et al., 2017). Additionally, the qRT-PCR analysis revealed a significant reduction of the *Cdh13* mRNA in the whole DR of *Cdh13* cKO when compared to Ctrl mice ($p<0.0001$) (Supplementary Fig. S1). Specifically, in the dorsal DR, where the anatomical locality allowed microdissection with the highest precision, the *Cdh13* mRNA level decreased approximately 66%. We assumed that the reduction was likely close to the latter estimation when we overcome the influence of the limited visualization methodology.

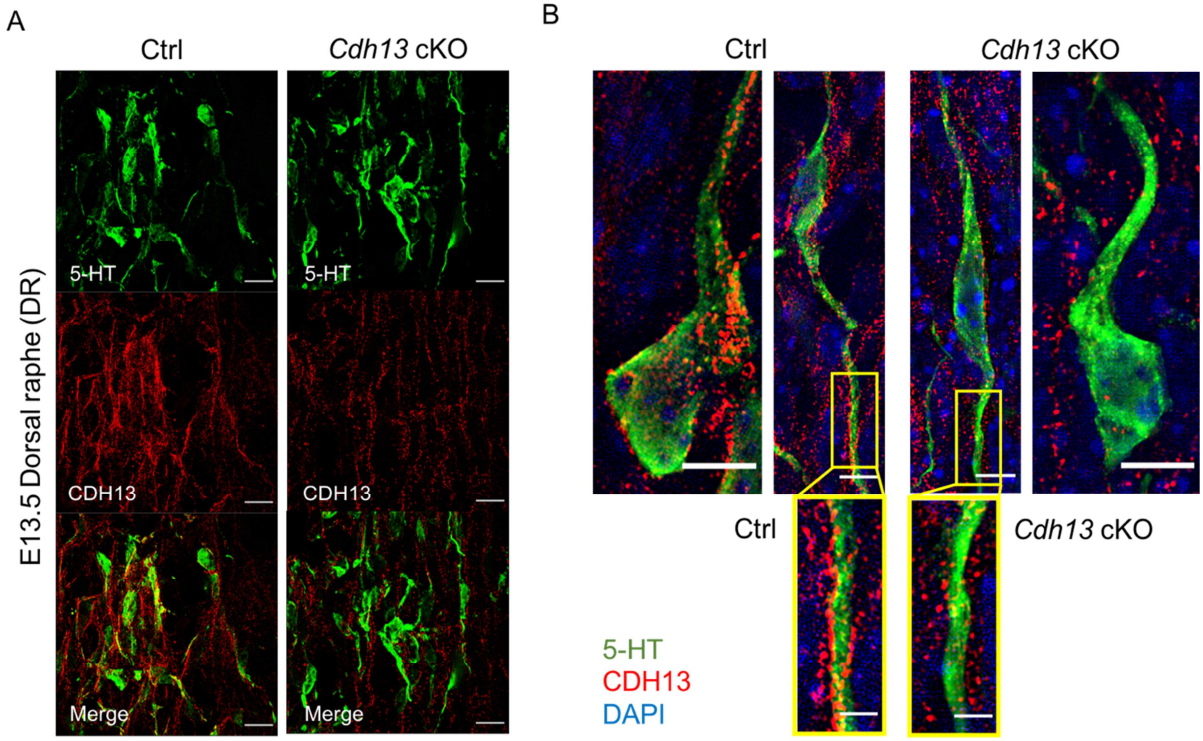

Figure 1. Immunofluorescence of CDH13 in 5-HT neurons in Ctrl vs. *Cdh13* cKO embryonic brains using structured illumination microscopy (SIM). (A) CDH13 immunoreactivity in the DR is considerably lower in *Cdh13* cKO animals compared to Ctrls. (B) At a cellular level, CDH13 does not cluster along 5-HT neuron extensions in *Cdh13* cKO brains compared to Ctrls. Orientation: sagittal. Scale bars: (a) 10 µm, (b) 5 µm; close-up 2 µm.

Once the loss of CDH13 in serotonergic neurons was confirmed in *Cdh13* cKO animals, an initial quantification of the density of 5-HT neurons was performed in the DR at E13.5. We observed a significant increase in 5-HT positive neuron density in *Cdh13* cKO embryos. While Ctrl littermates present an average of $8x10^{-5}$ cells/μm^3, *Cdh13* cKO mice have a density of approximately $11x10^{-5}$ cells/μm^3 (*P*=0.0138, Fig. 2). No significant difference in area occupied was found in DR between *Cdh13* cKO and Ctrl.

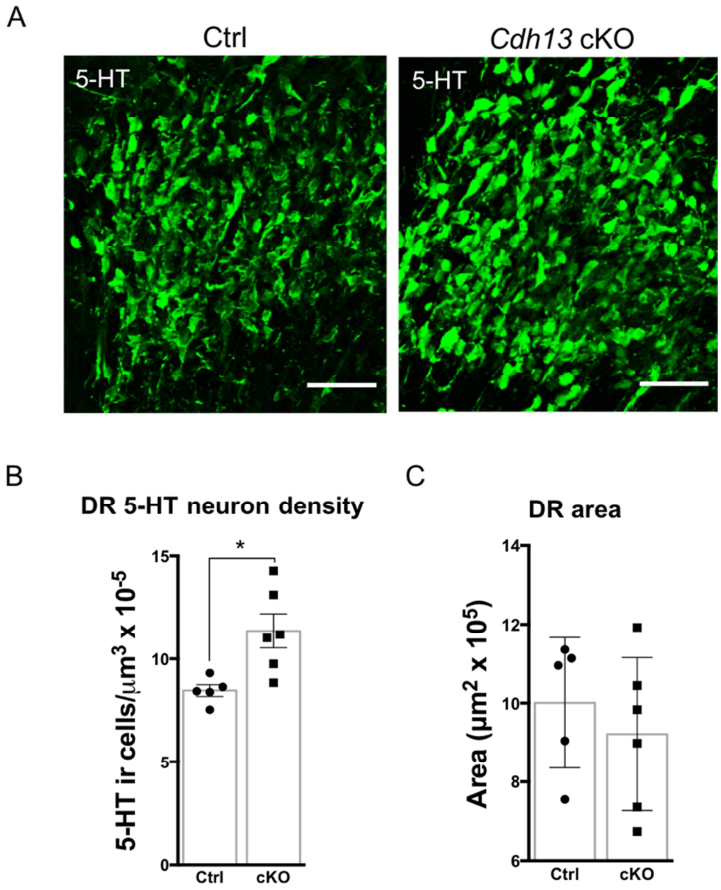

Figure 2. Dorsal raphe (DR) 5-HT neuron density and area at E13.5. (A) Representative images of the DR stained with 5-HT antibody show an increase in 5-HT neuron density in *Cdh13* cKO embryonic brains compared to Ctrl littermates. (B) A quantification of these cells reveals a significant increase of 5-HT positive neurons (Ctrl, n=5; *Cdh13* cKO, n=6; *P*=0.0138). (C) No difference in the area occupied by 5-HT positive neurons at E13.5 between *Cdh13* cKO and Ctrls (Ctrl, n=5; *Cdh13* cKO, n=6; *P*=0.489). Orientation: sagittal. Scale bar 50 µm. Data presented as mean ± s.e.m. **P*<0.05.

3.2. CDH13 deficiency restricted to *Pet1*-positive neurons increases serotonergic innervation of cortical regions during embryonic stages

The increase in 5-HT neuron density in the developing DR of *Cdh13* cKO directed us to investigate serotonergic innervation of the cortex at a later developmental stage (E17.5) when the fibers have reached cortical areas (Forero et al., 2017). By E17.5, 5-HT specific afferents

are observed to extend along two cortical layers, the marginal (MZ) and intermediate (IZ) zones. Our results show that the absence of CDH13 in serotonergic neurons results in an increase of 5-HT positive fibers in the developing cortex. We measured the area occupied by these fibers in two regions: (1) the prefrontal cortex (PFC) that will become a relevant cortical region in cognitive functioning and (2) the somatosensory cortex (SSC) that is shown to be highly affected by 5-HT system alterations during cortical development (Teissier, Soiza-Reilly, & Gaspar, 2017). In both areas, a significant difference between Ctrl and *Cdh13* cKO mice was identified (PFC: P=0.0403; SSC: P=0.0114; Fig. 3).

Coherent with the increased serotonergic innervation of the PFC, HPLC analysis revealed a significant increase of 5-HT levels in the PFC of *Cdh13* cKO embryos at E17.5, when compared to Ctrl littermates (P=0.049; Supplementary Fig. S2). No differences in 5-HT levels were observed in the raphe of those animals, however.

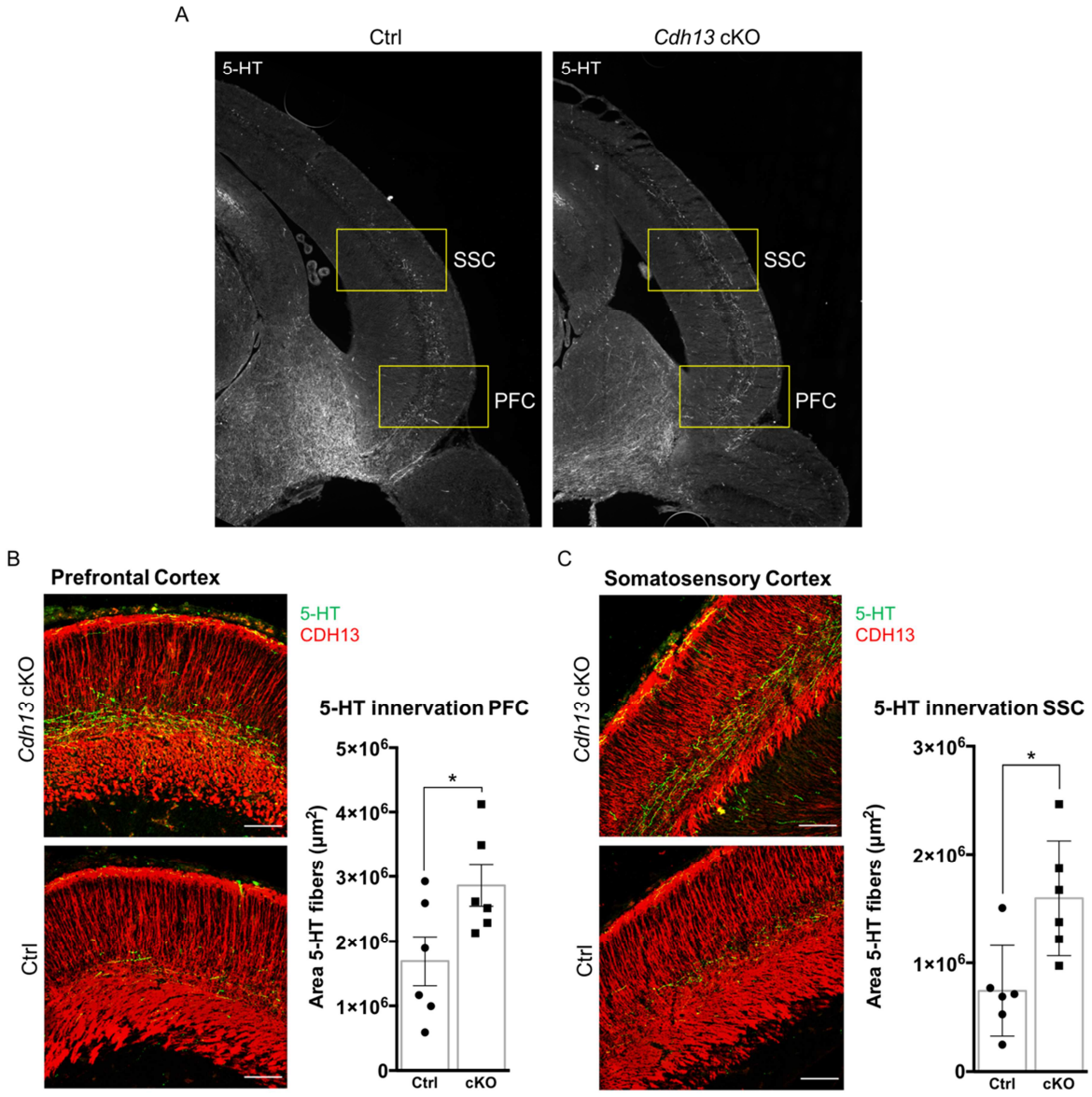

Figure 3. Serotonergic innervation in the prefrontal (PFC) and somatosensory (SSC) cortical areas at E17.5. (A) Sagittal sections of E17.5 forebrain. (B) Representative images of CDH13 and 5-HT expression in the PFC. *Cdh13* cKO mice show a significant increase in 5-HT innervation of the PFC compared to Ctrl

littermates (n=6 per genotype; *P*=0.0403). (B) Representative images of CDH13 and 5-HT expression in the SSC. *Cdh13* cKO mice also show a significant increase in 5-HT innervation of the SSC compared to Ctrl littermates (n=6 per genotype; *P*=0.0114). Orientation: sagittal. Scale bar 100 μm. Data presented as mean ± s.e.m. **P*<0.05.

3.3.CDH13 inactivation in serotonergic neurons differentially alters the number of Tph2-positive neurons in subgroups of the adult dorsal raphe nucleus

We next investigated whether the effects on 5-HT neuron density observed in the embryonic DR of *Cdh13* cKO persist into adulthood. Due to the heterogeneity in the identity and projection of the cells constituting the adult DR nucleus, a more detailed quantification of Tph2-positive neurons in this region was carried out. We analyzed three subgroups of the DR nucleus: the dorsal DR (B7d), the ventral DR (B7v) and the lateral DR (B7l). These DR areas had previously been identified to carry the main groups of cells projecting to our target regions of interest (Muzerelle et al., 2016).

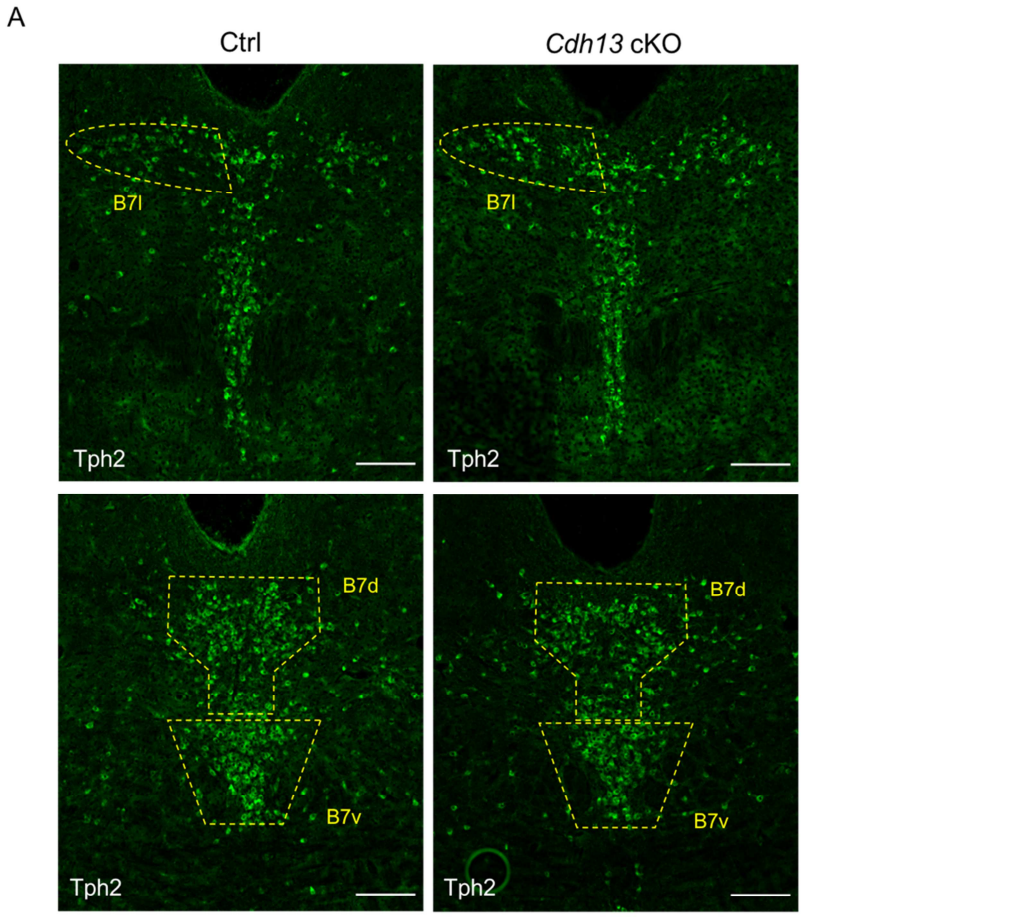
A
Ctrl
Cdh13 cKO
B7l
B7l
Tph2
Tph2
B7d
B7d
B7v
B7v
Tph2
Tph2

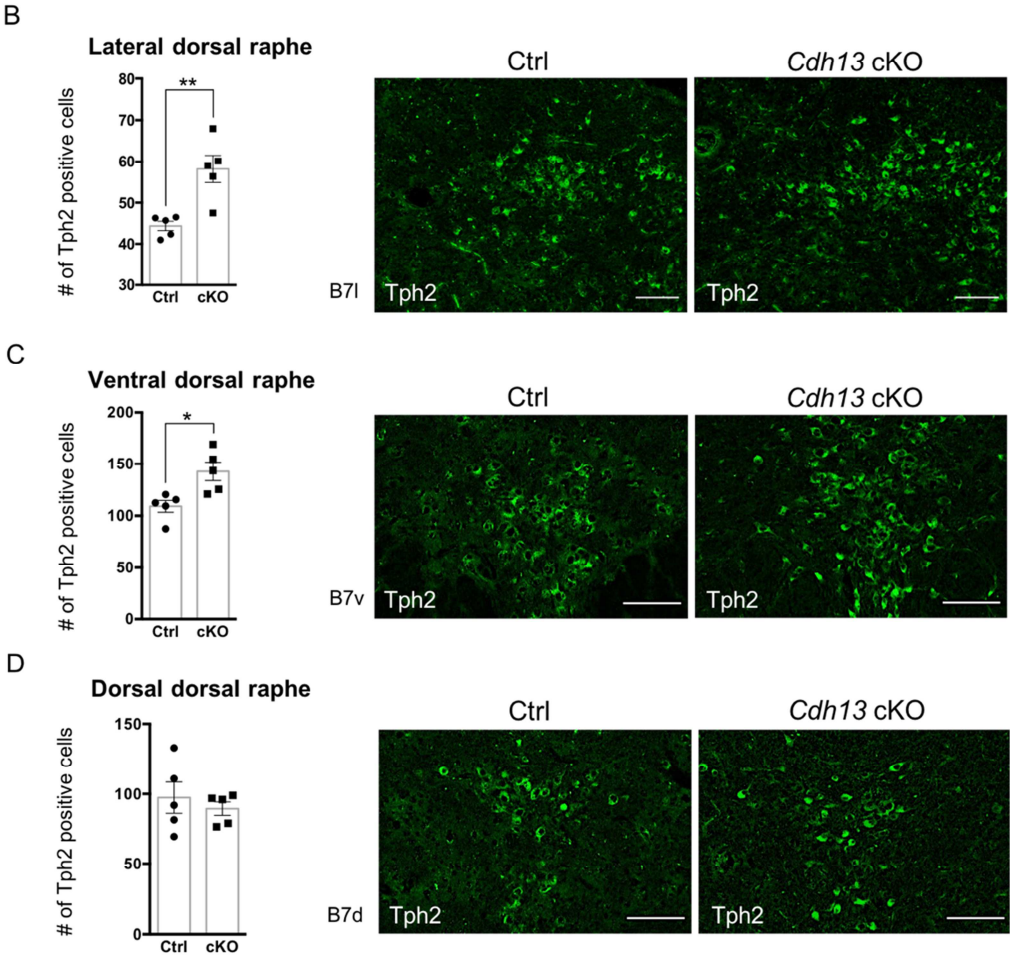
B
Lateral dorsal raphe
# of Tph2 positive cells
**
Ctrl
cKO
Ctrl
Cdh13 cKO
B7l
Tph2
Tph2
C
Ventral dorsal raphe
# of Tph2 positive cells
*
Ctrl
cKO
Ctrl
Cdh13 cKO
B7v
Tph2
Tph2
D
Dorsal dorsal raphe
# of Tph2 positive cells
Ctrl
cKO
Ctrl
Cdh13 cKO
B7d
Tph2
Tph2

Figure 4. Quantification of Tph2-positive neurons in the lateral (B7l), ventral (B7v) and dorsal (B7d) subregions of the adult dorsal raphe. (A) Locations of B7l, B7v and B7d in the DR. Yellow lines delimit the nuclei that were evaluated. (B,C) *Cdh13* cKO mice significantly differ in the cell density of B7l (A; n=5 per genotype; *P*=0.0041) and B7v (B; n=5 per genotype; *P*=0.0132), showing a higher cell number compared to Ctrl mice. (C) No differences in cell density were observed in the dorsal DR (B7d). Orientation: sagittal. Scale bars: (a) 200 μm (b, c) 100 μm. Data presented as mean ± s.e.m. **P*<0.05, ***P*<0.01.

Our results show that the number of serotonergic neurons is differentially altered in these DR subgroups (Fig. 4). Specifically, we observed an increase in Tph2-positive neurons in the lateral and ventral DR regions of *Cdh13* cKO mice compared to Ctrl littermates, while no difference was detected in the dorsal DR subregion.

3.4. Altered serotonergic innervation of forebrain regions targeted by the ventral (B7v) subregion of the dorsal raphe nucleus in conditional *Cdh13* knockouts

Anterograde tracing previously identified the lateral thalamus, mammillary bodies, superior colliculus, and facial cranial nerve as the main targets of the lateral DR, while the frontal and prefrontal cortex, amygdala, piriform cortex, and olfactory bulb were identified as targets of the ventral DR (Muzerelle et al., 2016). The differential alteration in the number of Tph2-positive neurons we observed in the lateral and ventral DR subgroups led us to analyze corresponding serotonergic innervation target regions. From these regions, we chose to analyze the lateral thalamus, prefrontal cortex, caudate putamen and amygdala.

Notably, our results show that the serotonergic innervation of some of these regions is affected in *Cdh13* cKO mice (Supplementary Fig. S3). Particularly, we observed a significantly altered innervation in the cingulate cortex and a trend towards significance in the amygdala; both of them are mainly B7v target regions.

3.5. *Cdh13* deficiency restricted to serotonergic neurons is associated to alterations in learning and impulsivity

Cdh13 cKO mice were subjected to a battery of behavioral tests with the aim to evaluate how 5-HT neuron-specific CDH13 deficiency affects locomotor activity, anxiety-like behavior, learning and memory as well as social behavior. The analysis revealed no significant genotype effects on anxiety-like behavior, assessed through the elevated plus maze (EPM), the light/dark box (LDB) and the open field (OF) tests. No difference was detected in the time spent in the center versus the borders in the OF (Fig. 5A), in the light versus dark compartment in the LDB (Fig. 5B), and in the open arms compared to closed arms in the EPM (Fig. 5C). Similarly, the total distance travelled in all tests mentioned above did not vary significantly between *Cdh13* cKO and Ctrl mice (Supplementary Fig. S4).

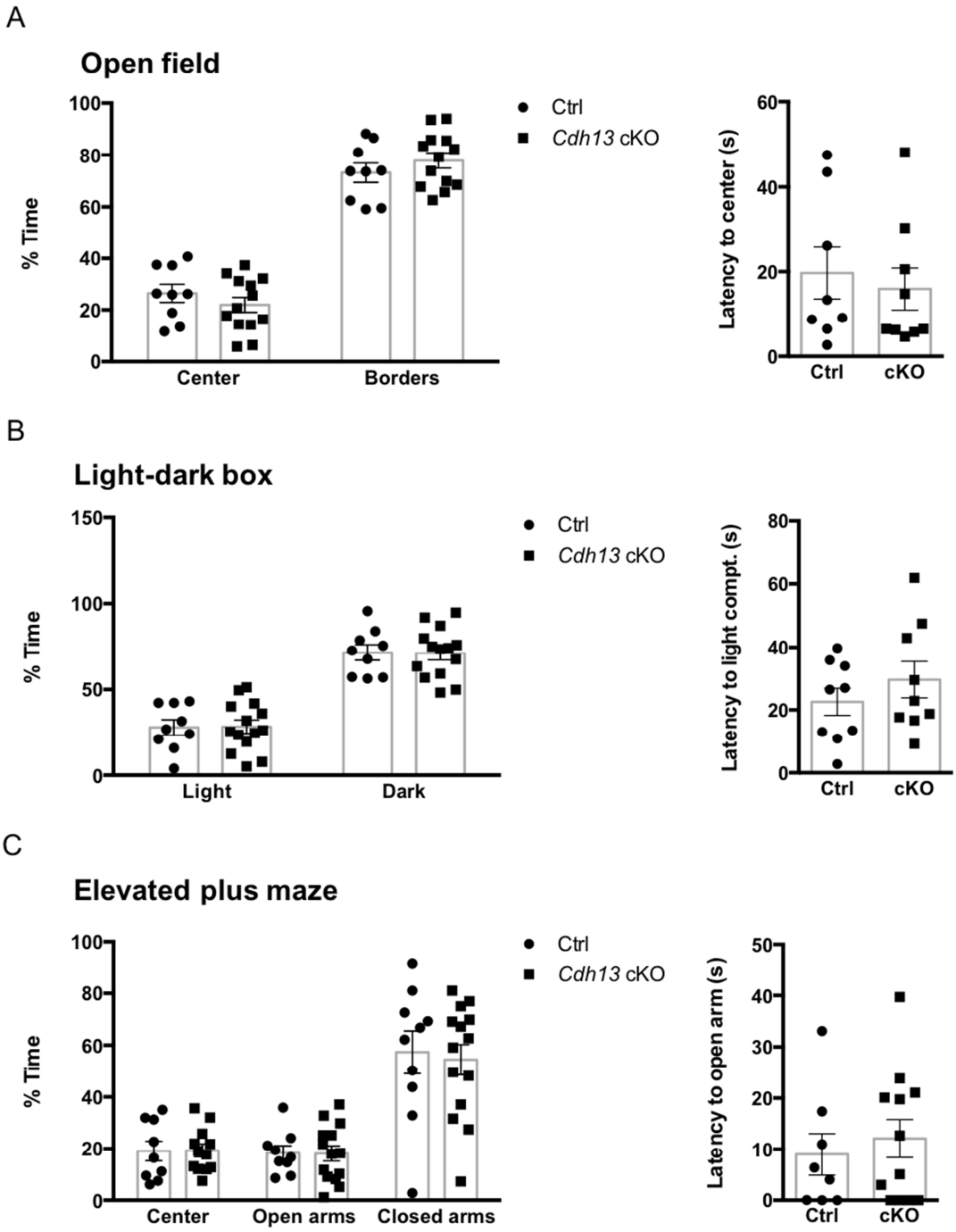

Figure 5. Behavioral assessment of anxiety-like behavior in *Cdh13* cKO mice. No significant differences were observed between Ctrl and *Cdh13* cKO mice in the open field test (A; Ctrl, n=9; *Cdh13* cKO, n=13), light-dark box (B; Ctrl, n=9; *Cdh13* cKO, n=14), and elevated plus maze (C; Ctrl, n=9; *Cdh13* cKO, n=14). Data presented as mean ± s.e.m.

The Barnes Maze (BM) was used to assess deficits in visuospatial learning and memory. Our results show that all mice were able to learn to find the escape hole within the allocated time. Both groups of mice spent more than a chance level of 25% of their time in the target quadrant during all stages, indicating that they had intact memory to remember the general location of the escape hole (Supplementary Fig. S5 and S6). However, there is a clear delay in the learning process of the *Cdh13* cKO mice. We observed an increased number of primary errors made during the early phases of training, more specifically in the second and fourth

days (Fig. 6A; Day 2 P= 0.0066; Day 4 P= 0.0086). Similar effect was observed, in the first trial after a 24 h intermission (Fig. 6A; Day 5 P= 0.0297). However, this difference is no longer detectable in the final days of testing, with the *Cdh13* cKO mice committing the same number of errors as the Ctrl animals. Additionally, we observed that *Cdh13* cKO mice have a significantly shorter latency to start carrying out the task compared to Ctrl animals both in the initial testing phase as well as in the testing phase after the 24-hour pause (Fig. 6B; Acquisition *P*= 0.014; Testing *P*= 0.001). As we could not observe a locomotor-initiation phenotype in the open field test, the here observed shorter latency might suggest increased impulsivity or motivation to start exploration.

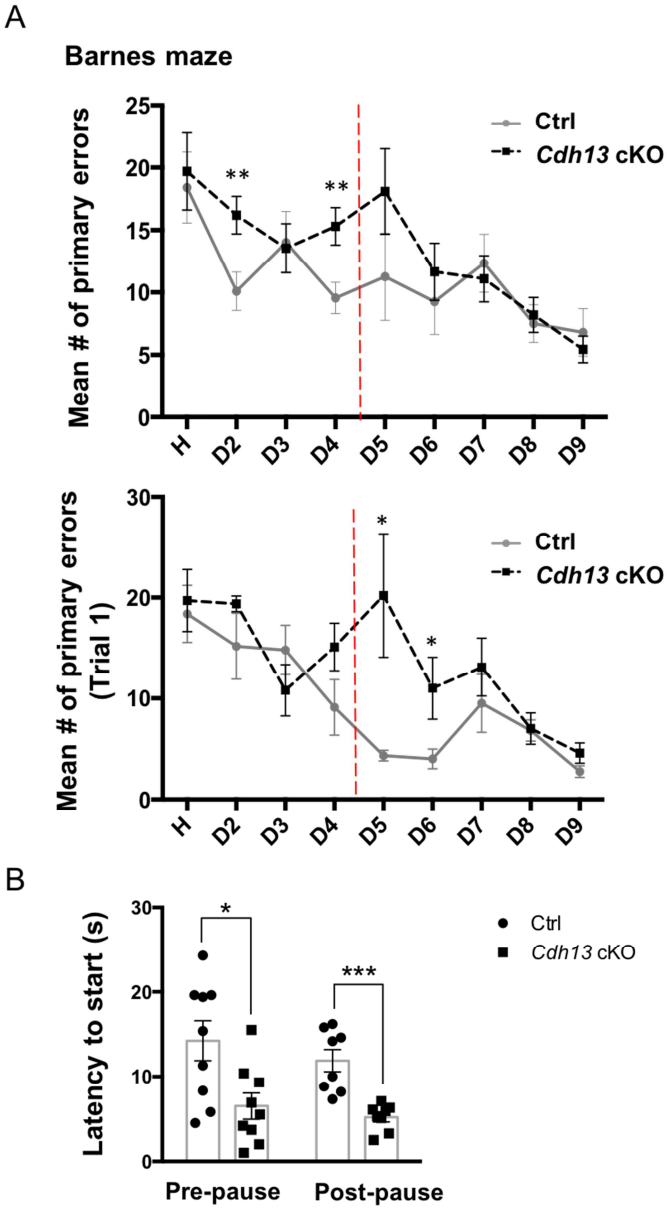

Figure 6. Behavioral assessment of visuospatial learning and memory through the Barnes Maze (BM). (A) A significant increase in the number of primary errors committed by the *Cdh13* cKO mice compared to Ctrl animals is observed in early stages (n=10 per genotype; D2 *P*= 0.0066; D4 *P*= 0.0086), as well as, in the first trials after a 24h break (n=10 per genotype; D5 *P*= 0.0297; D6 *P*= 0.0411; 24 h intermission represented by red dotted line). (B) *Cdh13* cKO mice show a significant decrease in the latency to start exploring both in the pre-pause (n=9 per genotype; *P*= 0.014) and post-pause (n=8 per genotype; *P*=0.001) phases. Data presented as mean ± s.e.m. **P*<0.05, ***P*<0.01, ****P*<0.001.

In order to assess deficits in social interaction and social recognition memory in the *Cdh13* cKO mice, we next applied a social interaction test, which consists of two consecutive paradigms that evaluate sociability and social novelty preference. During the first trial (sociability; Fig 7A), as expected, mice spent more time interacting with the cage containing a mouse rather than with the empty cage, although no genotype differences were detected. Nevertheless, a difference in the latency to interact with the animal/cage was observed, with *Cdh13* cKO mice being significantly quicker to start exploring the unfamiliar mouse (*P*= 0.0085). In addition, a tendency to a reduced latency to explore the empty cage was also observed in *Cdh13* cKOs (*P*= 0.0523). Like the BM results, this reduced latency may suggest either increased impulsivity and/or increased motivation to explore new environments. During the second trial performed 30 mins later (social novelty preference; Fig. 7B), all mice regardless of genotype spent longer time with the novel mouse rather than with the familiar mouse, indicating that social recognition memory was intact in the *Cdh13* cKO mice.

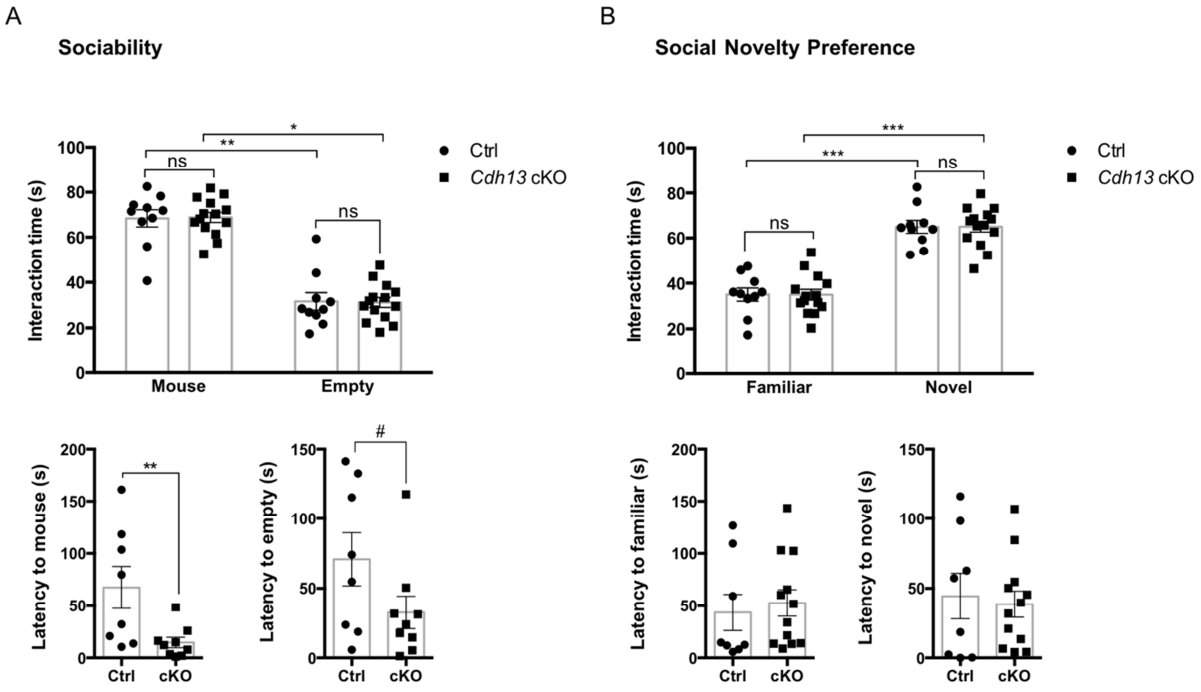

Figure 7. Assessment of social interaction in *Cdh13* conditional knockout mice. (A, B) No genotype difference is observed in sociability and social novelty preference between *Cdh13* cKO and Ctrl mice (Ctrl, n=10; cKO, n=14). However, *Cdh13* cKO do present a significantly reduced latency to interact with the test animal in the sociability test compared to Ctrl animals (Ctrl, n=8; *Cdh13* cKO, n=9; *P*= 0.0085), as well as, a tendency in the latency to explore the cage presented (Ctrl, n=8; *Cdh13* cKO, n=9; *P*= 0.0523). Data presented as mean ± s.e.m. #*P*<0.1, **P*<0.05, ***P*<0.01, ****P*<0.001.

Given the association between *Cdh13* and ADHD, as well as the findings presented above suggesting increased impulsivity, we determined visuospatial attentional performance and motor impulsivity using the 5-CSRTT paradigm (Fig. 8). Mice were trained to acquire the task through different stages and only when they reached >75% accuracy and <15% omissions in three consecutive days at a StD of 10 s, they entered the testing phase where the StD was reduced to 5 and 2 s, followed by two final sessions of variable ITI challenges.

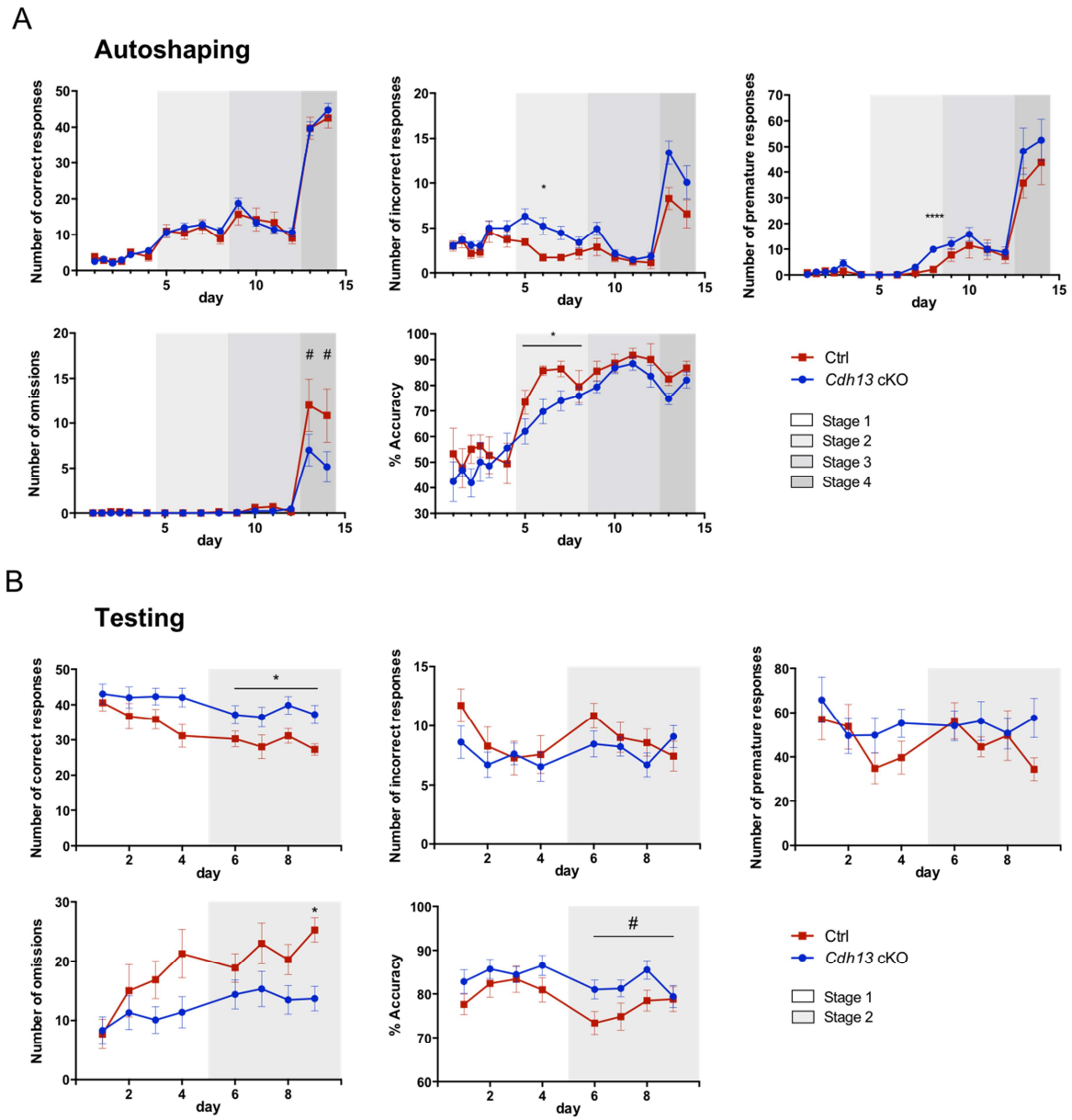

Figure 8. Assessment of attentional performance and motor impulsivity in *Cdh13* cKO mice with the 5-CSRTT. (A) During the second stage of autoshaping, *Cdh13* cKO mice made significantly more incorrect responses (genotype: $F_{1,18}$ = 7.984, p = 0.0112; D6: p = 0.0135) and premature responses (genotype x session: $F_{3,54}$ = 12.29, p < 0.0001; D8: p < 0.0001) compared to Ctrl littermates. Meanwhile, the percentage of accuracy during the same autoshaping stage decreased significantly in *Cdh13* cKO mice (genotype: $F_{1,18}$ = 5.319, p = 0.0332). (B) In contrast, *Cdh13* cKO mice performed better than the Ctrls in the testing phase. Session x genotype interactions for the number of correct responses ($F_{3,54}$ = 5.480; p = 0.0023) and omissions ($F_{3,54}$ = 5.323; p = 0.0028) were found in stage one. Genotype effects for the number of correct responses (genotype: $F_{1,18}$ = 5.133; p = 0.0360) and omissions (genotype: $F_{1,18}$ = 4.745; p = 0.0429) were detected in the subsequent stage. (Ctrl, n=7; *Cdh13* cKO, n=13). Data were analyzed by two-way mixed-design ANOVA and presented as mean ± s.e.m. #*P*<0.1, **P*<0.05, ***P*<0.01, ****P*<0.001.

Foremost, we compared the overall performance of both genotypes during the autoshaping phase by pooling all autoshaping sessions and stages together. We had a closer look at the learning curves and the performance in testing by analyzing independently the individual stages of the autoshaping (Fig. 8A and Supplementary Fig. S9) and testing (Fig. 8B and Supplementary Fig. S10) phases, respectively.

This analysis revealed that CDH13-deficient mice showed a delay in the learning process compared to their Ctrl counterparts, supported by an increased number of incorrect responses (genotype: $F_{1,18} = 7.984$, $p = 0.0112$; D6: $p = 0.0135$) in stage two while the number of correct response remained unaltered, which correspondingly led to a lower choice accuracy (genotype: $F_{1,18} = 5.319$, $p = 0.0332$). Additionally, increased premature responses (genotype × session: $F_{3,54} = 12.29$, $p < 0.0001$; D8: $p < 0.0001$) in the same stage indicate that they had difficulties restraining themselves from responding prematurely to the stimuli, an indicator of impulsive behavior. Despite the delay, *Cdh13* cKO mice were able to eventually acquire the task and performed similar to Ctrl animals in the last two autoshaping stages.

However, the analysis of the testing phase showed that when the StD is reduced to 5 s and 2 s (paired with 10 s of ITI), the CDH13-deficient mice displayed more sustained attention relative to the Ctrl littermates. In stage one (StD = 5 s), session × genotype interactions for the number of correct responses ($F_{3,54} = 5.480$; $p = 0.0023$) and omissions ($F_{3,54} = 5.323$; $p = 0.0028$) were found. Following this, genotype main effects for these two measures (correct responses: $F_{1,18} = 5.133$; $p = 0.0360$; omissions: $F_{1,18} = 4.745$; $p = 0.0429$) were detected in the subsequent stage (StD = 2s). This is due to the fact that the performance of *Cdh13* cKO mice remained constant across different durations of the stimulus while the performance of the Ctrl group became worse (Supplementary Table S4 and S5). Additionally, the *Cdh13* cKO mice made more nose-pokes, which reached a significant level only in testing stage two (genotype x session: $F_{3,54} = 4.347$, $p = 0.0082$; D8: $p = 0.0246$). No differences were found for other parameters such as incorrect responses, accuracy, and premature responses. Interestingly, in spite of varying the ITI duration in the challenge sessions, the performance of both groups was similar (Supplementary Fig. S11).

4. Discussion

The study we present here shows how *Cdh13* deficiency exclusively in 5-HT neurons is sufficient to modify the development of the brain 5-HT system. *Cdh13* cKO increases 5-HT neuron density in the embryonic DR, and serotonergic hyperinnervation of the developing prefrontal cortex. In the adult brain, *Cdh13* deficiency exclusively affects the 5-HT neuron density in the lateral (B7l) and ventral (B7v) subregions of the DR as well as the innervation of the cingulate cortex, a region specifically targeted by the ventral DR subgroup. At the behavioral level, adult *Cdh13* cKO mice display delayed acquisition of several learning tasks and a subtle impulsive-like phenotype, with decreased latency in the sociability paradigm alongside with deficits in visuospatial memory. Changes in anxiety-related traits were not observed in the conditional knockout mice. The cellular alterations in the 5-HT network might be responsible for the cognitive deficits and other behavioral features observed in *Cdh13* cKO mice.

The brain 5-HT system is of considerable relevance to numerous neurodevelopmental and psychiatric conditions, due to its regulatory role in basic cellular processes, such as migration

and differentiation of neurons (Gaspar et al., 2003; Lesch & Waider, 2012), but also in the development and plasticity of other transmission systems (Whitaker-Azmitia, 2001). Therefore, the search for modulators of 5-HT neuron development and function is fundamental in neurobiology. We had previously reported that CDH13 is strongly expressed in serotonergic neurons of the embryonic and adult mouse DR (Forero et al., 2017; Rivero et al., 2013). Particularly, the localization of CDH13 in 5-HT neuron/radial glia interaction sites points to a potential role of CDH13 in regulation of 5-HT neuron migration in the DR. In agreement with this notion, we could show how constitutive inactivation of CDH13 led to a significant increase in the 5-HT cell density of the DR nucleus at embryonic and adult stages, as well as a serotonergic hyperinnervation of the prefrontal cortex in embryonic stages (Forero et al., 2017). However, the differences we observed in full CDH13 knockout mice could not be specifically attributed to the presence of CDH13 in 5-HT neurons.

Here, the conditional *Cdh13* knockout mouse served as a practical tool for an initial screening of the relationship between CDH13 specifically in serotonergic neurons and the 5-HT system. Notably, serotonergic specific *Cdh13* conditional knockout mice display alterations in the 5-HT DR system (i.e. increased 5-HT neuron density) that are similar to those observed in the constitutive KO mice. Therefore, we provide evidence that adequate formation of this serotonergic nucleus is directly affected by CDH13 expression, and even though we may hypothesize that other factors are also involved in early prenatal neurodevelopmental processes, the absence of CDH13 alone from 5-HT expressing neurons is sufficient to lead to morphological and behavioral consequences.

Cdh13 cKO embryos also display serotonergic hyperinnervation of the developing cortex. Cadherins are known to be one of the many molecular cues that provide assistance to establish functional neural circuits through guidance of axons to their specific targets during development (Van Battum, Brignani, & Pasterkamp, 2015). However, to our knowledge, only a few members of this superfamily have been implied in serotonergic neuron development in the context of proper target-specific innervation by projecting fibers (Forero et al., 2017; Hayano et al., 2014; Katori et al., 2009; Katori et al., 2017). In this regard, protocadherin-α is strongly expressed in 5-HT neurons, while its specific deficiency from the 5-HT neurons leads to abnormal distribution of 5-HT projections in several brain regions (Katori et al., 2017; Katori et al., 2009). Similarly, our results indicate that absence of CDH13 in the 5-HT system enhances the serotonergic innervation in the prefrontal cortex, a brain region that plays a critical role in executive function and decision making. Considering the link between *CDH13* and ASD vulnerability, these findings are in agreement with the increase in 5-HT transporter-immunoreactive axons observed in the cortex of ASD patients (Azmitia, Singh, & Whitaker-Azmitia, 2011).

An effect of the serotonergic hyperinnervation observed in *Cdh13* cKO embryos appears to be the increase of 5-HT levels in cortical areas. Notably, hyperserotoninemia is one of the most reliable biomarkers in ASD (Ruggeri, Sarkans, Schumann, & Persico, 2014). Although it is not clear which are the consequences that this increased level of serotonin has on ASD pathophysiology, the effects of elevated serotonin levels during early neurodevelopment have

been extensively studied using 5-HT transporter (*Slc6a4*)-deficient mice. The lifelong increase of extracellular 5-HT in cortical regions detected in those mice (Fox et al., 2007; Mathews et al., 2004) leads to an abnormal distribution of GABAergic interneurons in the cerebral cortex (Riccio et al., 2009), which may affect the excitatory-inhibitory balance of brain circuits, one of the underlying mechanisms that have been proposed for several neurodevelopmental disorders (Marin, 2012; Penzes, Buonanno, Passafaro, Sala, & Sweet, 2013; Selten, van Bokhoven, & Nadif Kasri, 2018). Given the existing link between CDH13 deficiency and alterations in the GABAergic system (Paradis et al., 2007; Rivero et al., 2015; Tantra et al., 2018), it would be of utmost relevance to further study the interaction between the serotonergic and GABAergic systems in the *Cdh13* cKO mouse

Complementary to our investigations of the embryonic brain, we also aimed to clarify how the effects of CDH13 deficiency in 5-HT neurons persisted in the adult brain and ultimately, how behavior was affected. Because the alterations in 5-HT neuron density were only restricted to the lateral and ventral subregions of the adult DR and given the specific properties of each DR serotonin subsystem (Ren et al., 2018) , we subsequently quantified 5-HTT innervation in multiple brain regions that are known to be innervated by these two DR subnuclei (Muzerelle et al., 2016). Contrary to our expectations, we observed that serotonergic innervation was significantly reduced in the cingulate cortex of *Cdh13* cKO mice and unchanged in the infralimbic cortex. Although difficult to explain without any additional data, we speculate that there are compensatory mechanisms in the developing cortex of conditional KO mice that counterbalance the effects produced by CDH13 deficiency and might lead to reduced innervation when adulthood is reached. Serotonergic PFC innervation is shown to be a dynamic process which involves regulatory processes that decrease its density and generate changes in fiber and synapse morphology as age advances (Maddaloni et al., 2017). This same regulation might be involved in the shift that we observe from 5-HT hyperinnervation in late embryonic stages to largely normal innervation in the adult prefrontal cortex and subcortical regions in *Cdh13* cKO mice. In addition, considering the key role of homophilic interactions for cadherin function, the different levels of CDH13 expression throughout the mouse brain (Rivero et al., 2013) might help to understand the variability in the effects induced by CDH13 deficiency in serotonergic fibers.

Correlating with the structural changes in the DR-related serotonergic network, behavioral assessment revealed that the conditional deletion of CDH13 in the 5-HT system also had an effect on the acquisition in the Barnes Maze test, a visuo-spatial learning paradigm, and the 5-CSRTT, a task developed to screen for attention deficits and increased impulsivity. Contrasting this effect on learning paradigms, *Cdh13* cKO mice did not differ from controls with respect to locomotor activity or anxiety-like behavior. This finding also agrees with the view of neurodevelopmental disorders as complex conditions where different (genetic and/or environmental) risk factors may mediate specific aspects of the disorder (in this case, cognitive dimensions).

The delayed learning and memory acquisition in *Cdh13* cKO mice is analogous to the moderate learning deficits that are widely reported in ADHD patients (McCann & Roy-Byrne,

2000), and also very similar to the learning deficits we observed in mice with a constitutive inactivation of CDH13 (Rivero et al., 2015). This similarity supports the view that the effect of CDH13 on cognition is largely mediated by its role in serotonergic function, although the (direct or indirect) influence from other systems (e.g. GABAergic) should be considered.

Notably, *Cdh13* cKO mice display behavior that may be interpreted as a result of increased impulsivity-like traits. With the battery of behavioral tests conducted, we were able to identify two essential features of impulsivity (Pattij & Vanderschuren, 2008) in our mice. Particularly, *Cdh13* cKO mice exhibited a shortened response latency in the BM and the sociability/social novelty preference test. In addition, in the training phase of the 5-CSRTT, *Cdh13* cKO mice made more premature responses, an effect that was not observed once the task was acquired, however. The impulsive-like behaviors we observed may be associated with the altered serotonergic innervation in the cingulate cortex. The integrity and balanced transmission in the anterior cingulate cortex (ACC) are important for inhibitory response control (Hvoslef-Eide et al., 2018), while the extracellular levels of 5-HT in the medial PFC are positively correlated to the premature responses in the 5-CSRTT (Dalley & Roiser, 2012) as well as in the delay discounting task (Winstanley, Theobald, Dalley, Cardinal, & Robbins, 2006). However, further investigation is needed to clarify the existence of a link between the observed impulsive-like phenotype and the detected molecular and cellular changes in the ACC.

Rather unexpectedly, despite the delay in acquiring the 5-CSRTT, *Cdh13* cKO mice performed better during the testing phases, in terms of more correct responses and less omissions. This enhanced performance exhibited by *Cdh13* cKO mice may be an indicator of sustained attention and/or higher level of motivation (i.e. hyperfocus, widely described in ADHD patients; Hupfeld, Abagis, and Shah (2019)). The lack of evidence on attention deficits during the autoshaping phase would however favor the idea that *Cdh13* cKO mice display enhanced motivation which allows them to perform better over the whole testing phase. Indeed, the PFC has been implicated in the activation of mesolimbic dopaminergic areas to induce reward-motivated behavior (Ballard et al., 2011). However, the involvement of serotonergic PFC circuits in motivation or sustained attention remains largely unknown.

In conclusion, we show that inactivation of CDH13 specifically in *Pet1*-positive (serotonergic) neurons correlates with an increased density of 5-HT neurons in the developing DR and in specific subnuclei of the adult DR, as well as changes in serotonergic innervation of the developing PFC. Furthermore, our results support CDH13 as a pivotal element for the development of the brain 5-HT system, by showing that absence of CDH13 exclusively in serotonergic neurons is sufficient to alter cell density and innervation in specific target areas. Notably, conditional CDH13 deficiency is also enough to induce specific cognitive alterations in adult mice that correlate with the specific clinical features observed in neurodevelopmental and psychiatric disorders.

5. Acknowledgements

We gratefully recognize the excellent technical assistance of G. Ortega y Schulte, N. Steigerwald, and A. Dietzel. We also thank C. Rüdt von Collenberg for her support with the laser-capture microdissection method. This work was supported by Deutsche Forschungsgemeinschaft (DFG: SFB TRR 58/A5, to KPL), the European Union's Seventh Framework Programme (FP7/2007–2013) under Grant No. 602805 (Aggressotype), the Horizon 2020 Research and Innovation Programme under Grant No. 728018 (Eat2beNICE) and Grant No. 643051 (MiND), ERA-Net NEURON/RESPOND, No. 01EW1602B, ERA-Net NEURON/DECODE, No. 01EW1902 (to KPL and OR) and 5-100 Russian Academic Excellence Project (to KPL). AF was supported by a grant of the German Excellence Initiative to the Graduate School of Life Sciences (GSLS), University of Würzburg. The funding entities had no role in the study design, data collection and analysis, decision to publish or preparation of the manuscript.

6. References

Attar, A., Liu, T., Chan, W. T., Hayes, J., Nejad, M., Lei, K., & Bitan, G. (2013). A shortened Barnes maze protocol reveals memory deficits at 4-months of age in the triple-transgenic mouse model of Alzheimer's disease. *PLoS One, 8*(11), e80355. doi:10.1371/journal.pone.0080355

Azmitia, E. C., Singh, J. S., & Whitaker-Azmitia, P. M. (2011). Increased serotonin axons (immunoreactive to 5-HT transporter) in postmortem brains from young autism donors. *Neuropharmacology, 60*(7-8), 1347-1354. doi:10.1016/j.neuropharm.2011.02.002

Ballard, I. C., Murty, V. P., Carter, R. M., MacInnes, J. J., Huettel, S. A., & Adcock, R. A. (2011). Dorsolateral prefrontal cortex drives mesolimbic dopaminergic regions to initiate motivated behavior. *J Neurosci, 31*(28), 10340-10346. doi:10.1523/JNEUROSCI.0895-11.2011

Ciatto, C., Bahna, F., Zampieri, N., VanSteenhouse, H. C., Katsamba, P. S., Ahlsen, G., . . . Shapiro, L. (2010). T-cadherin structures reveal a novel adhesive binding mechanism. *Nat Struct Mol Biol, 17*(3), 339-347. doi:10.1038/nsmb.1781

Dai, J. X., Han, H. L., Tian, M., Cao, J., Xiu, J. B., Song, N. N., . . . Xu, L. (2008). Enhanced contextual fear memory in central serotonin-deficient mice. *Proc Natl Acad Sci U S A, 105*(33), 11981-11986. doi:10.1073/pnas.0801329105

Dalley, J. W., & Roiser, J. P. (2012). Dopamine, serotonin and impulsivity. *Neuroscience, 215*, 42-58. doi:10.1016/j.neuroscience.2012.03.065

Deneris, E., & Gaspar, P. (2018). Serotonin neuron development: shaping molecular and structural identities. *Wiley Interdiscip Rev Dev Biol, 7*(1). doi:10.1002/wdev.301

Forero, A., Rivero, O., Waldchen, S., Ku, H. P., Kiser, D. P., Gartner, Y., . . . Lesch, K. P. (2017). Cadherin-13 Deficiency Increases Dorsal Raphe 5-HT Neuron Density and Prefrontal Cortex Innervation in the Mouse Brain. *Front Cell Neurosci, 11*, 307. doi:10.3389/fncel.2017.00307

Fox, M. A., Andrews, A. M., Wendland, J. R., Lesch, K. P., Holmes, A., & Murphy, D. L. (2007). A pharmacological analysis of mice with a targeted disruption of the serotonin transporter. *Psychopharmacology (Berl), 195*(2), 147-166. doi:10.1007/s00213-007-0910-0

Fredette, B. J., Miller, J., & Ranscht, B. (1996). Inhibition of motor axon growth by T-cadherin substrata. *Development, 122*(10), 3163-3171.

Fredette, B. J., & Ranscht, B. (1994). T-cadherin expression delineates specific regions of the developing motor axon-hindlimb projection pathway. *J Neurosci, 14*(12), 7331-7346.

Gaspar, P., Cases, O., & Maroteaux, L. (2003). The developmental role of serotonin: news from mouse molecular genetics. *Nat Rev Neurosci, 4*(12), 1002-1012. doi:10.1038/nrn1256

Gustafsson, M. G. (2000). Surpassing the lateral resolution limit by a factor of two using structured illumination microscopy. *J Microsc, 198*(Pt 2), 82-87.

Gutknecht, L., Kriegebaum, C., Waider, J., Schmitt, A., & Lesch, K. P. (2009). Spatio-temporal expression of tryptophan hydroxylase isoforms in murine and human brain: convergent data from Tph2 knockout mice. *Eur Neuropsychopharmacol, 19*(4), 266-282. doi:10.1016/j.euroneuro.2008.12.005

Gutknecht, L., Waider, J., Kraft, S., Kriegebaum, C., Holtmann, B., Reif, A., . . . Lesch, K. P. (2008). Deficiency of brain 5-HT synthesis but serotonergic neuron formation in Tph2 knockout mice. *J Neural Transm (Vienna), 115*(8), 1127-1132. doi:10.1007/s00702-008-0096-6

Hawi, Z., Tong, J., Dark, C., Yates, H., Johnson, B., & Bellgrove, M. A. (2018). The role of cadherin genes in five major psychiatric disorders: A literature update. *Am J Med Genet B Neuropsychiatr Genet, 177*(2), 168-180. doi:10.1002/ajmg.b.32592

Hayano, Y., Zhao, H., Kobayashi, H., Takeuchi, K., Norioka, S., & Yamamoto, N. (2014). The role of T-cadherin in axonal pathway formation in neocortical circuits. *Development, 141*(24), 4784-4793. doi:10.1242/dev.108290

Hendricks, T. J., Fyodorov, D. V., Wegman, L. J., Lelutiu, N. B., Pehek, E. A., Yamamoto, B., . . . Deneris, E. S. (2003). Pet-1 ETS gene plays a critical role in 5-HT neuron development and is required for normal anxiety-like and aggressive behavior. *Neuron, 37*(2), 233-247. doi:10.1016/s0896-6273(02)01167-4

Hupfeld, K. E., Abagis, T. R., & Shah, P. (2019). Living "in the zone": hyperfocus in adult ADHD. *Atten Defic Hyperact Disord, 11*(2), 191-208. doi:10.1007/s12402-018-0272-y

Hvoslef-Eide, M., Nilsson, S. R., Hailwood, J. M., Robbins, T. W., Saksida, L. M., Mar, A. C., & Bussey, T. J. (2018). Effects of anterior cingulate cortex lesions on a continuous performance task for mice. *Brain Neurosci Adv, 2*. doi:10.1177/2398212818772962

Katori, S., Hamada, S., Noguchi, Y., Fukuda, E., Yamamoto, T., Yamamoto, H., . . . Yagi, T. (2009). Protocadherin-alpha family is required for serotonergic projections to appropriately innervate target brain areas. *J Neurosci, 29*(29), 9137-9147. doi:10.1523/JNEUROSCI.5478-08.2009

Katori, S., Noguchi-Katori, Y., Okayama, A., Kawamura, Y., Luo, W., Sakimura, K., . . . Yagi, T. (2017). Protocadherin-alphaC2 is required for diffuse projections of serotonergic axons. *Sci Rep, 7*(1), 15908. doi:10.1038/s41598-017-16120-y

Killen, A. C., Barber, M., Paulin, J. J. W., Ranscht, B., Parnavelas, J. G., & Andrews, W. D. (2017). Protective role of Cadherin 13 in interneuron development. *Brain Struct Funct, 222*(8), 3567-3585. doi:10.1007/s00429-017-1418-y

Kiyasova, V., Fernandez, S. P., Laine, J., Stankovski, L., Muzerelle, A., Doly, S., & Gaspar, P. (2011). A genetically defined morphologically and functionally unique subset of 5-HT neurons in the mouse raphe nuclei. *J Neurosci, 31*(8), 2756-2768. doi:10.1523/JNEUROSCI.4080-10.2011

Kiyasova, V., & Gaspar, P. (2011). Development of raphe serotonin neurons from specification to guidance. *Eur J Neurosci, 34*(10), 1553-1562. doi:10.1111/j.1460-9568.2011.07910.x

Lesch, K. P., & Waider, J. (2012). Serotonin in the modulation of neural plasticity and networks: implications for neurodevelopmental disorders. *Neuron, 76*(1), 175-191. doi:10.1016/j.neuron.2012.09.013

Maddaloni, G., Bertero, A., Pratelli, M., Barsotti, N., Boonstra, A., Giorgi, A., . . . Pasqualetti, M. (2017). Development of Serotonergic Fibers in the Post-Natal Mouse Brain. *Front Cell Neurosci, 11*, 202. doi:10.3389/fncel.2017.00202

Marin, O. (2012). Interneuron dysfunction in psychiatric disorders. *Nat Rev Neurosci, 13*(2), 107-120. doi:10.1038/nrn3155

Mathews, T. A., Fedele, D. E., Coppelli, F. M., Avila, A. M., Murphy, D. L., & Andrews, A. M. (2004). Gene dose-dependent alterations in extraneuronal serotonin but not dopamine in mice with reduced serotonin transporter expression. *J Neurosci Methods, 140*(1-2), 169-181. doi:10.1016/j.jneumeth.2004.05.017

McCann, B. S., & Roy-Byrne, P. (2000). Attention-deficit/hyperactivity disorder and learning disabilities in adults. *Semin Clin Neuropsychiatry, 5*(3), 191-197.

Muzerelle, A., Scotto-Lomassese, S., Bernard, J. F., Soiza-Reilly, M., & Gaspar, P. (2016). Conditional anterograde tracing reveals distinct targeting of individual serotonin cell groups (B5-B9) to the forebrain and brainstem. *Brain Struct Funct, 221*(1), 535-561. doi:10.1007/s00429-014-0924-4

Okaty, B. W., Freret, M. E., Rood, B. D., Brust, R. D., Hennessy, M. L., deBairos, D., . . . Dymecki, S. M. (2015). Multi-Scale Molecular Deconstruction of the Serotonin Neuron System. *Neuron, 88*(4), 774-791. doi:10.1016/j.neuron.2015.10.007

Paradis, S., Harrar, D. B., Lin, Y., Koon, A. C., Hauser, J. L., Griffith, E. C., . . . Greenberg, M. E. (2007). An RNAi-based approach identifies molecules required for glutamatergic and GABAergic synapse development. *Neuron, 53*(2), 217-232. doi:10.1016/j.neuron.2006.12.012

Pattij, T., & Vanderschuren, L. J. (2008). The neuropharmacology of impulsive behaviour. *Trends Pharmacol Sci, 29*(4), 192-199. doi:10.1016/j.tips.2008.01.002

Penzes, P., Buonanno, A., Passafaro, M., Sala, C., & Sweet, R. A. (2013). Developmental vulnerability of synapses and circuits associated with neuropsychiatric disorders. *J Neurochem, 126*(2), 165-182. doi:10.1111/jnc.12261

Philippova, M., Ivanov, D., Allenspach, R., Takuwa, Y., Erne, P., & Resink, T. (2005). RhoA and Rac mediate endothelial cell polarization and detachment induced by T-cadherin. *FASEB J, 19*(6), 588-590. doi:10.1096/fj.04-2430fje

Ranscht, B., & Bronner-Fraser, M. (1991). T-cadherin expression alternates with migrating neural crest cells in the trunk of the avian embryo. *Development, 111*(1), 15-22.

Ren, J., Friedmann, D., Xiong, J., Liu, C. D., Ferguson, B. R., Weerakkody, T., . . . Luo, L. (2018). Anatomically Defined and Functionally Distinct Dorsal Raphe Serotonin Sub-systems. *Cell, 175*(2), 472-487 e420. doi:10.1016/j.cell.2018.07.043

Riccio, O., Potter, G., Walzer, C., Vallet, P., Szabo, G., Vutskits, L., . . . Dayer, A. G. (2009). Excess of serotonin affects embryonic interneuron migration through activation of the serotonin receptor 6. *Mol Psychiatry, 14*(3), 280-290. doi:10.1038/mp.2008.89

Rivero, O., Selten, M. M., Sich, S., Popp, S., Bacmeister, L., Amendola, E., . . . Lesch, K. P. (2015). Cadherin-13, a risk gene for ADHD and comorbid disorders, impacts GABAergic function in hippocampus and cognition. *Transl Psychiatry, 5*, e655. doi:10.1038/tp.2015.152

Rivero, O., Sich, S., Popp, S., Schmitt, A., Franke, B., & Lesch, K. P. (2013). Impact of the ADHD-susceptibility gene CDH13 on development and function of brain networks. *Eur Neuropsychopharmacol, 23*(6), 492-507. doi:10.1016/j.euroneuro.2012.06.009

Robbins, T. W. (2002). The 5-choice serial reaction time task: behavioural pharmacology and functional neurochemistry. *Psychopharmacology (Berl), 163*(3-4), 362-380. doi:10.1007/s00213-002-1154-7

Ruggeri, B., Sarkans, U., Schumann, G., & Persico, A. M. (2014). Biomarkers in autism spectrum disorder: the old and the new. *Psychopharmacology (Berl), 231*(6), 1201-1216. doi:10.1007/s00213-013-3290-7

Schatz, D. B., & Rostain, A. L. (2006). ADHD with comorbid anxiety: a review of the current literature. *J Atten Disord, 10*(2), 141-149. doi:10.1177/1087054706286698

Selten, M., van Bokhoven, H., & Nadif Kasri, N. (2018). Inhibitory control of the excitatory/inhibitory balance in psychiatric disorders. *F1000Res, 7*, 23. doi:10.12688/f1000research.12155.1

Tantra, M., Guo, L., Kim, J., Zainolabidin, N., Eulenburg, V., Augustine, G. J., & Chen, A. I. (2018). Conditional deletion of Cadherin 13 perturbs Golgi cells and disrupts social and cognitive behaviors. *Genes Brain Behav, 17*(6), e12466. doi:10.1111/gbb.12466

Teissier, A., Soiza-Reilly, M., & Gaspar, P. (2017). Refining the Role of 5-HT in Postnatal Development of Brain Circuits. *Front Cell Neurosci, 11*, 139. doi:10.3389/fncel.2017.00139

Van Battum, E. Y., Brignani, S., & Pasterkamp, R. J. (2015). Axon guidance proteins in neurological disorders. *Lancet Neurol, 14*(5), 532-546. doi:10.1016/S1474-4422(14)70257-1

Wegel, E., Gohler, A., Lagerholm, B. C., Wainman, A., Uphoff, S., Kaufmann, R., & Dobbie, I. M. (2016). Imaging cellular structures in super-resolution with SIM, STED and Localisation Microscopy: A practical comparison. *Sci Rep, 6*, 27290. doi:10.1038/srep27290

Whitaker-Azmitia, P. M. (2001). Serotonin and brain development: role in human developmental diseases. *Brain Res Bull, 56*(5), 479-485. doi:10.1016/s0361-9230(01)00615-3

Winstanley, C. A., Theobald, D. E., Dalley, J. W., Cardinal, R. N., & Robbins, T. W. (2006). Double dissociation between serotonergic and dopaminergic modulation of medial prefrontal and orbitofrontal cortex during a test of impulsive choice. *Cereb Cortex, 16*(1), 106-114. doi:10.1093/cercor/bhi088

Wyler, S. C., Donovan, L. J., Yeager, M., & Deneris, E. (2015). Pet-1 Controls Tetrahydrobiopterin Pathway and Slc22a3 Transporter Genes in Serotonin Neurons. *ACS Chem Neurosci, 6*(7), 1198-1205. doi:10.1021/cn500331z

Wyler, S. C., Spencer, W. C., Green, N. H., Rood, B. D., Crawford, L., Craige, C., . . . Deneris, E. (2016). Pet-1 Switches Transcriptional Targets Postnatally to Regulate Maturation of Serotonin Neuron Excitability. *J Neurosci, 36*(5), 1758-1774. doi:10.1523/JNEUROSCI.3798-15.2016

Exclusive inactivation of CDH13 in 5-HT neurons selectively increases 5-HT neuron density in the embryonic brain and adult dorsal raphe nucleus.

Conditional deletion of CDH13 in 5-HT neurons also increases serotonergic innervation of developing cortical regions in the mouse embryonic brain

Adult Cdh13 cKO mice display delayed acquisition of several learning tasks and a subtle impulsive-like phenotype.